# Channel Inversion Method for Optimum Power Delivery in RF Harvesting Backscatter Systems

***Abstract*—This work presents a method for enhanced wireless power transfer using an algorithm to calculate the optimum phases of multiple transmitting antennas in a passive UHF RFID system. The algorithm performs the calculation based on measured backscatter phase value of individual antenna port and the phase rotation caused by each port's receiving channel. Through experimental validations, it is shown that the proposed algorithm can achieve up to 18 dB improvement in the tag RSSI using three transmitting antennas. The proposed algorithm could be used in the next generation sensor tags to optimise power delivery efficiency.**

***Index Terms*—Radio propagation, UHF measurements, UHF propagation, Radiofrequency identification**

## I. Introduction

With the development of the Internet of Things (IoT), an increasing number of sensors are being deployed. According to a report by ARM, the amount of IoT modules being produced may reach 1 trillion between 2017 and 2035, among which up to 75% could be wireless and operate without on-board power supplies [1]. The adoption of battery-less sensors significantly reduces the cost of deployment and maintenance. Moreover, without batteries, those sensors have a longer lifetime and are more friendly to the environment [2].

However, the wide deployment of battery-less sensors also poses a tremendous challenge to the wireless power transfer (WPT) techniques which usually provide a small amount of power to electronic devices reliably within a few metres [2]. One of the most common application scenarios is in passive Ultra High Frequency Radio Frequency Identification (UHF RFID), where tags operate through harvesting the reader transmit power and respond through backscatter modulation [2]. The turn-on power for a state-of-the-art RFID integrated circuit (IC) is around -24 dBm [3], [4]. At this sensitivity level, according to the Friis equation [5], with an effective isotropic radiated power (EIRP) of 36 dBm, ideally the tag IC can be activated at more than 20 metres away from the transmit antenna at 866 MHz. However, due to the complexity in operating environments, such a range is rarely, if ever achieved in practice. For tags with integrated sensors, a much higher turn-on power will be required in most applications [6], [7]. For instance, a power level of -12 dBm will limit the operating range to less than 5 metres. This range could be further shortened by multi-path interferences, polarisation mismatches, and poor impedance matching performances when tags are placed near metallic objects [8].

As a result, many techniques have been proposed in the literature to enhance the power delivery to tags. Among those techniques, some focus on developing novel beam-scanning antennas to enhance the system coverage by steering the antenna beam to different directions [9]–[11]; some work in [12], [13] attempts to achieve a wide-area coverage through the usage of a distributed antenna system (DAS) combined with frequency and phase hopping. Those techniques have been successful in combating multi-path effects and are sufficient for improving the detection probability of conventional passive RFID tags. However, sensor tags have different operational requirements, as not only is the power requirement much higher, they must also be polled regularly.

In addition to exploiting the spatial diversity in a multi-antenna system, several beam-forming techniques have been proposed to further improve the amount of power delivered to sensor tags [14]–[17]. However, most of those techniques are based on blind adaptive beam-forming (BABF) or its variants where the initial transmitting phases are randomly chosen while the optimal phase combination is searched iteratively. When the number of transmitting antennas is large, those methods' convergence speed is expected to be slow.

In this work, an algorithm to calculate the optimal phase combination for a multi-antenna RFID system is proposed, tested and verified. The proposed algorithm can directly compute the optimal phase combination based on some pre-calibrated parameters and a few initial inventories, eliminating the lengthy process in conventional iterative search methods. A series of experiments have shown that a local power improvement of over 18 dB in the received tag backscatter power is achieved between the optimal and worst phase combinations. Although not yet available, we make the assumption that a sensor tag can be developed to suit our system where backscatter communication to enable channel measurements can be carried out with a much lower threshold power than sensing itself.

In summary, the contributions of this paper are:

1) We propose a simple yet effective algorithm for distributed beam-forming in passive UHF RFID in which the optimal phase combination can be directly computed without using iterative searching methods.
2) We present comprehensive experimental data from a real-life test configuration and verify that the experimental data well matches the theoretical analysis.

The rest of this paper is organised as follows: Section II presents the analysis of the proposed algorithm. The experiment set-up, including the hardware design and calibration, is detailed in Section III. Section IV presents the measurement results of the proposed algorithm and an analysis of it. Finally, conclusions are drawn in Section V.

## II. A Phase-based Beam-forming Technique for UHF RFID

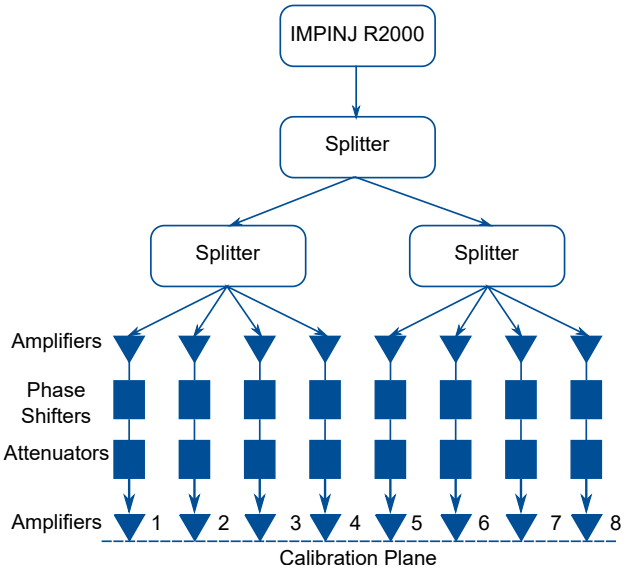


Fig. 1. Architecture of the reader prototype based on Indy R2000 [18]

Fig. 1 shows the diagram of our multi-channel reader prototype with independent control of power and phase at each port. The reader has eight antenna ports, each of which can be configured as either a transmitting or a receiving channel. When used as a transmitter, the on board $360^\circ$ phase shifter and two power amplifiers are enabled. A digital attenuator with a 30 dB dynamic range is used to adjust the output power to meet local power requirement. The reader operates in bi-static mode, with up to seven transmitting antennas can be used for beam-forming, while the remaining antenna functions as the receiver.

To demonstrate how the transmit phases should be optimised, consider the scenario in which port 1 is used as the receiving port while port 2 and port 3 are used as the transmitting ports. The proposed algorithm's target is to find the correct phase combination for port 2 and port 3 such that both ports' electromagnetic fields result in constructive interference at the target tag location. To determine the correct phases, we exploit the reciprocal nature of the channel and start with port 1 initially set as the transmitter. The received phases at ports 2 and 3 can be expressed as:

$$\begin{aligned} \mathrm{P2}_{rx} &= a_1 + a_2 + c_2 + \varphi_{BS2} \\ \mathrm{P3}_{rx} &= a_1 + a_3 + c_3 + \varphi_{BS3} \end{aligned} \tag{1}$$

where $a_1$ is the phase rotation introduced in the channel between port 1 and the target tag; $a_2$ and $a_3$ are the phase changes caused by the channel from the tag to port 2 and port 3 respectively; $c_2$ and $c_3$ are fixed phase rotations associated with the receiving channel of port 2 or port 3 (from the corresponding port's input to the IC of the reader and can be found by calibration using a VNA); $\varphi_{BS2}$ and $\varphi_{BS3}$ are the backscatter phases of tag modulation, which are dependent on the incident power [19]. To ensure that the signals arrived at the tag from ports 2 and 3 are in phase, the target transmitting phases $\mathrm{P2}_{tx}$ and $\mathrm{P3}_{tx}$ of port 2 and port 3 should satisfy:

$$\mathrm{P2}_{tx} + a_2 + \varphi'_{BS2} = \mathrm{P3}_{tx} + a_3 + \varphi'_{BS3} \tag{2}$$

By adding $a_1$ to both sides, we have:

$$\mathrm{P2}_{tx} + a_1 + a_2 + \varphi'_{BS2} = \mathrm{P3}_{tx} + a_1 + a_3 + \varphi'_{BS3} \tag{3}$$

The following equation can be obtained by substituting equation 1 into equation 3 and assume that $\varphi_{BS2}$ and $\varphi_{BS3}$ are equal to $\varphi'_{BS2}$ and $\varphi'_{BS3}$:

$$\mathrm{P2}_{tx} + \mathrm{P2}_{rx} - c_2 = \mathrm{P3}_{tx} + \mathrm{P3}_{rx} - c_3 \tag{4}$$

As a result:

$$\mathrm{P3}_{tx} = \mathrm{P2}_{tx} + \mathrm{P2}_{rx} - c_2 + c_3 - \mathrm{P3}_{rx} \tag{5}$$

From equation 5, it is clear that by setting port 2 as the phase reference (so that $\mathrm{P2}_{tx} = 0^\circ$), the optimum transmitting phase of port 3 ($\mathrm{P3}_{tx}$) can be directly calculated once $c_2$ and $c_3$ are determined.

The algorithm can easily be expanded by adding more transmitting antennas. With one transmitting antenna being added, only a single measurement is needed to obtain the corresponding received phase $\mathrm{Pi}_{rx}$. Then, the transmitting phase of that antenna can be calculated by substituting the antenna index $i$ into equation 5:

$$\mathrm{Pi}_{tx} = \mathrm{P2}_{tx} + \mathrm{P2}_{rx} - c_2 + c_i - \mathrm{Pi}_{rx} \tag{6}$$

With the transmitting phase of each port being calculated, the best phase combination $P_b$ can be denoted as (with port 1 being the receiving antenna while port 2 being the phase reference):

$$\mathrm{P}_b = [0 \ \mathrm{P3}_{tx} \ \mathrm{P4}_{tx} \ \ldots \ \mathrm{Pi}_{tx}] \tag{7}$$

After the best phase combination is known, the worst phase combination can be calculated using algorithm 1 (with 3 transmitting antennas as an example). In the algorithm, sort(sqrt(lin(RSSI))) means to convert the received RSSI into the linear format, do square root and sort it in ascending order. $\theta_1$ and $\theta_2$ are the two positive roots of equation 8 using vector calculations, as indicated in Fig. 2:

$$\begin{aligned} R_{lin}(1) \cdot \sin(\theta_1) &= R_{lin}(2) \cdot \sin(\theta_2) \\ R_{lin}(1) \cdot \cos(\theta_1) + R_{lin}(2) \cdot \cos(\theta_2) &= R_{lin}(3) \end{aligned} \tag{8}$$

We use the worst phase combination to validate our system, it could also be useful for physical tag suppression in real scenarios.

The proposed algorithm is computationally light and easy to achieve. The received phase $\mathrm{Pi}_{rx}$ of the target tag can be directly retrieved through tag inventories, while the phases of the receiving channel ($c_2$ and $c_3$) are fixed and can be obtained through calibrations as shown in the next section.

**Algorithm 1:** Worst Phase Combination

**Input:** The RSSI of port 2 3 and 4

**Output:** The worst phase combination $P_w$ of port 2 3 and 4, the best and worst RSSI ($R_b$ and $R_w$) in theory

**begin**

$R_{lin} \leftarrow$sort(sqrt(lin(RSSI)));

**if** $R_{lin}(1) + R_{lin}(2) < R_{lin}(3)$ **then**

$R_b \leftarrow (\text{sum}(R_{lin}))^2$;

$R_w \leftarrow R_{lin}(end) - \text{sum}(R_{lin}(1:2))$;

$P_w \leftarrow P_b + [180^\circ \ 180^\circ \ 0]$;

**else**

$R_b \leftarrow (\text{sum}(R_{lin}))^2$;

$R_w \leftarrow 0$;

$P_w \leftarrow P_b + [180^\circ - \theta_1 \ -(180^\circ - \theta_2) \ 0]$;

**end**

**end**

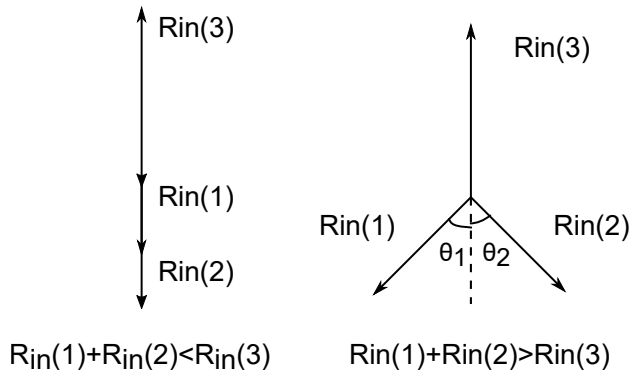


Fig. 2. Two different conditions in calculating the worst phase combination

## III. Experiment Configuration

To validate the proposed algorithm, a custom development board based on Impinj Indy R2000 evaluation module (EVM) [18] is used. The R2000 EVM output is connected to several power dividers to create 8 switch-able transmit/receive ports, each equipped with two power amplifiers, a 360° phase shifter and a digital attenuator. Each port's output phase and power can be manipulated by setting the corresponding registers in the micro-control unit (MCU).

### A. Port Calibration

Before any experiments are conducted, the system is calibrated to the calibration plane in Fig. 1 so that the phase values in the calculations are accurate and stable.

The output phase calibration is performed using the development board and a Rohde & Schwarz® ZVA67 vector network analyser (VNA) [20].

In the calibration process, the VNA's output is connected to each port's input while the input channel of the VNA is connected to the output of each channel. During the calibration, the 8-bit phase register of the port being calibrated is varied from 0 to 255 in steps of 1. The phase output value is queried for 16 times, and the average value is recorded. The phase calibration results are shown in Fig. 3.

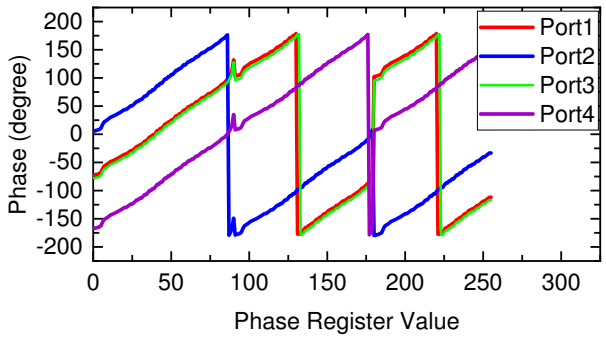


Fig. 3. Phase calibration results of port 1 to port 4 at the operating frequency of 865.7 MHz

To compensate the output phase variations caused by the change in the output power, stability calibration is performed for each port by keeping the phase register unchanged while varying the reader's attenuation register. The stability calibration results are shown in Fig. 4.

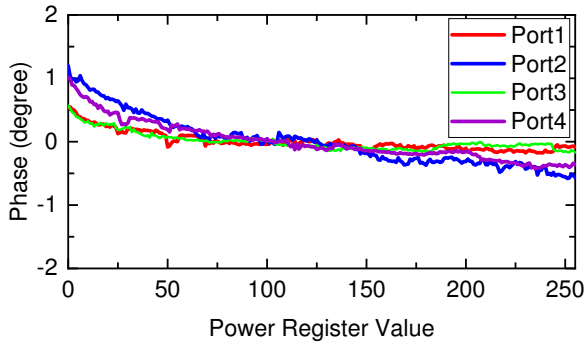


Fig. 4. Phase stability against output power of port 1 to port 4 at the operating frequency of 865.7 MHz. The mean value of each channel is removed to reveal the variations.

From Fig. 4, it is clear that the output phase of each channel is independent from its output power.

### B. Experiment Set-up

Fig. 5 shows the experimental setup. For proof-of-concept purposes, four reader antennas (MT-242021/NV/K [21]) are placed in a $3\text{m} \times 5\text{m}$ room facing the same direction. Among them, one antenna is connected to port 1 as the receiving antenna while three antennas are connected to port 2 to port 4 as transmitting antennas. Four highly sensitive, passive RFID tags [22] are hung on a rope and are placed around 2 metres away from the antennas. The distance between those four RFID tags is around 40 cm.

During the experiment, the operating frequency is fixed to a single value at 865.7 MHz to ensure the received phase's

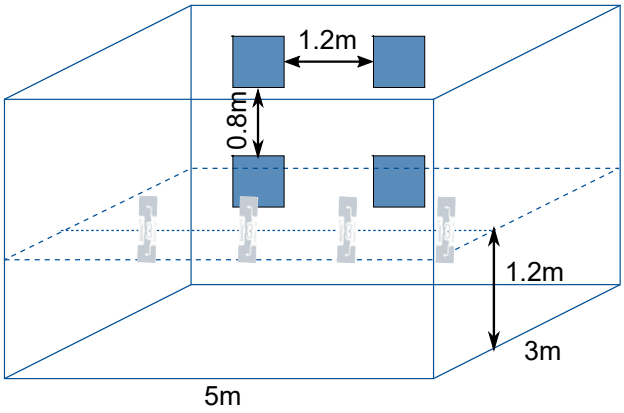


Fig. 5. The test environment

stability while the transmit power is set to a low level at 26 dBm ERP to ensure the linearity of tag's RSSI against its received power [23]. The experiment process follows the steps detailed in section II:

1) The received phases $\mathrm{P2}_{rx}$ $\mathrm{P3}_{rx}$, and $\mathrm{P4}_{rx}$ are found through inventories.
2) The best phase combination is found using equation 6.
3) The worst combination, the best and worst RSSI ($R_b$ and $R_w$) in theory, are decided using algorithm 1.

It is worth noting that the RFID reader chip used in the prototype (Impinj R2000 [18]) has a received phase ambiguity of $180°$ [24]. In equation 6, it is the phase difference between the reference port and the target port ($\mathrm{P2}_{rx} - \mathrm{Pi}_{rx}$) that matters, with a phase ambiguity of $180°$, the optimal phase value being found can either be the correct value $\mathrm{Pi}_{rx}$ or a false value $\mathrm{Pi'}_{rx} = \mathrm{Pi}_{rx} + 180°$. With 3 transmitting antennas, this would result in $2^{(3-1)} = 4$ possible optimal phase combinations.

This $180°$ phase ambiguity problem is caused by the internal phase-recovery methodology of the R2000 RFID reader chip [24] and would slightly affect the speed of the proposed algorithm. It can be eliminated by replacing the reader chip with a custom field-programmable gate array (FPGA) chip that implements an improved phase-recovered method such as the one in [25]. However, for proof-of-concept purposes, this problem is tolerated. We resolve this issue by testing all 4 possible combinations, and selecting the one with the highest RSSI value as the optimal phase combination. Once the optimum combination has been found, algorithm 1 is used to calculate the corresponding worst phase combination.

To test the algorithm, we attempt to optimise the power delivered to each of the 4 tags in turn. For each tag location, the algorithm runs 30 times to verify its stability.

## IV. Results

The received phase values of each channel against the attempt index are shown in Fig. 6. Each channel's $180°$ phase ambiguity is clearly shown in this figure as there are two groups of phases (low and high, in the same colour) for each channel. It is also clear that the received phase values remain stable during the experiments.

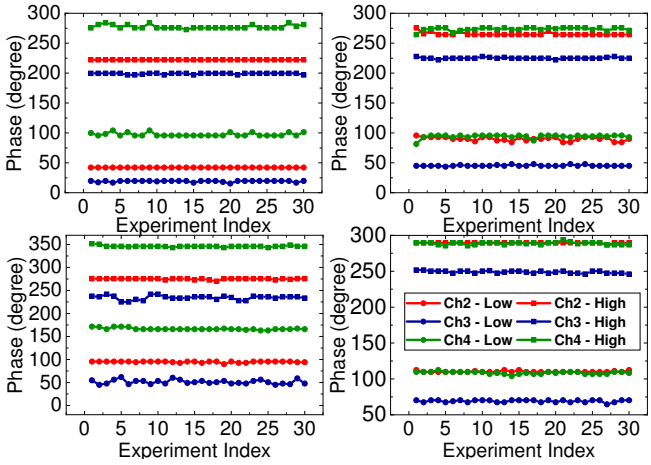


Fig. 6. The received phase of channels at 4 locations

The received RSSI values versus experiment index are shown in Fig. 7. If the reader cannot read the target tag, its RSSI is recorded as -90 dBm. For ease of comparison, the theoretical worst RSSI ($R_b$) is also denoted as -90 dBm, although in theory the value is close to $-\infty$.

Fig. 7 shows that the algorithm works well in optimising the received RSSI of tags. Depending on the tag's location, the difference in RSSI can vary up to 18 dB. This difference might be even higher, as in some experiments, the RSSI of the target tag is too low to be detected by the reader. It is also noticed that the best RSSI values obtained in the experiments are always a few decibels lower than the theoretical maximum. This phenomenon is likely to be caused by the fact that the backscatter phases $\varphi_{BS}$ and $\varphi'_{BS}$ in equation 1 and equation 3 are dependent on the target tag's incident power value and are not precisely the same. This problem can be alleviated by performing a phase search around the best phase combination.

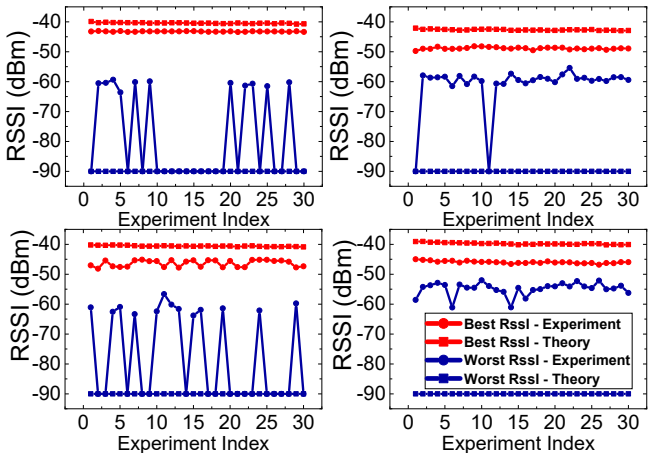


Fig. 7. The received RSSI versus experiment index of 4 locations.

## V. Conclusion

An algorithm which can quickly calculate the best phase combination of multiple transmitting antennas in a multi-antenna RFID system is proposed and experimentally verified. The proposed algorithm does not rely on iterative phase searching methods, avoiding slow convergence speed and can be implemented with low computational complexity. It is experimentally demonstrated that the proposed algorithm can achieve an RSSI improvement of up to 18 dB using three transmitting antennas. The proposed algorithm can easily be scaled up by adding more transmitting antennas and calculate the corresponding phase using a simple equation. This algorithm can be used on sensor tags to optimise the power delivery to RFID-based sensors.

## References


[1] P. Sparks, "The route to a trillion devices," *White Paper, ARM*, 2017.

[2] D. M. Dobkin, *The RF in RFID: UHF RFID in practice*. Newnes, 2012.

[3] Impinj. (2020, may) Impinj m730 & m750 product brief / datasheet. [Online]. Available: https://support.impinj.com/hc/en-us/articles/360010797539-Impinj-M730-M750-Product-Brief-Datasheet

[4] G. D. Durgin, "RF thermoelectric generation for passive RFID," in *2016 IEEE International Conference on RFID (RFID)*. IEEE, 2016, pp. 1–8.

[5] C. A. Balanis, *Antenna theory: analysis and design*. John wiley & sons, 2016.

[6] S. Naderiparizi, A. N. Parks, Z. Kapetanovic, B. Ransford, and J. R. Smith, "Wispcam: A battery-free RFID camera," in *2015 IEEE International Conference on RFID*, April 2015, pp. 166–173.

[7] B. Wang, M.-K. Law, J. Yi, C.-Y. Tsui, and A. Bermak, "A -12.3 dbm UHF passive RFID sense tag for grid thermal monitoring," *IEEE Transactions on Industrial Electronics*, vol. 66, no. 11, pp. 8811–8820, 2019.

[8] T. Björninen, L. Sydänheimo, L. Ukkonen, and Y. Rahmat-Samii, "Advances in antenna designs for UHF RFID tags mountable on conductive items," *IEEE Antennas and Propagation Magazine*, vol. 56, no. 1, pp. 79–103, 2014.

[9] R. Chen, S. Yang, A. M. Ndifon, I. H. White, R. V. Penty, and M. Crisp, "Beam scanning UHF RFID reader antenna with high gain and wide axial ratio beamwidth," *IEEE Journal of Radio Frequency Identification*, 2020.

[10] S.-L. Chen, P.-Y. Qin, W. Lin, and Y. J. Guo, "Pattern-reconfigurable antenna with five switchable beams in elevation plane," *IEEE Antennas and Wireless Propagation Letters*, vol. 17, no. 3, pp. 454–457, 2018.

[11] C. Liu, S. Xiao, Y.-X. Guo, Y.-Y. Bai, and B.-Z. Wang, "Broadband circularly polarized beam-steering antenna array," *IEEE Transactions on Antennas and Propagation*, vol. 61, no. 3, pp. 1475–1479, 2012.

[12] S. Sabesan, M. J. Crisp, R. V. Penty, and I. H. White, "Wide area passive UHF RFID system using antenna diversity combined with phase and frequency hopping," *IEEE Transactions on Antennas and Propagation*, vol. 62, no. 2, pp. 878–888, 2014.

[13] A. M. Ndifon, M. J. Crisp, R. V. Penty, and I. H. White, "Enhanced RFID tag detection accuracy using distributed antenna arrays," in *2018 IEEE International Conference on RFID (RFID)*, 2018, pp. 1–6.

[14] J. Wang, J. Zhang, R. Saha, H. Jin, and S. Kumar, *Pushing the range limits of commercial passive RFIDs*, 2019.

[15] S. Chen, S. Zhong, S. Yang, and X. Wang, "A Multiantenna RFID Reader with Blind Adaptive Beamforming," *IEEE Internet of Things Journal*, vol. 3, no. 6, pp. 986–996, 2016.

[16] X. Fan, H. Ding, S. Li, M. Sanzari, Y. Zhang, W. Trappe, Z. Han, and R. E. Howard, "Energy-Ball: Wireless Power Transfer for Batteryless Internet of Things through Distributed Beamforming," *Proceedings of the ACM on Interactive, Mobile, Wearable and Ubiquitous Technologies*, vol. 2, no. 2, pp. 1–22, jul 2018. [Online]. Available: https://dl.acm.org/doi/10.1145/3214268

[17] P. S. Yedavalli, T. Riihonen, X. Wang, and J. M. Rabaey, "Far-field rf wireless power transfer with blind adaptive beamforming for internet of things devices," *IEEE Access*, vol. 5, pp. 1743–1752, 2017.

[18] Impinj. (2019, oct) Indy R2000 RAIN RFID reader chip. [Online]. Available: https://www.impinj.com/platform/connectivity/indy-r2000/

[19] P. V. Nikitin, R. Martinez, S. Ramamurthy, H. Leland, G. Spiess, and K. V. S. Rao, "Phase based spatial identification of UHF RFID tags," in *2010 IEEE International Conference on RFID (IEEE RFID 2010)*, 2010, pp. 102–109.

[20] Rohde & Schwarz. (2020, jan) R&S ZVA vector network analyzers. [Online]. Available: https://www.rohde-schwarz.com/ca/product/zva-productstartpage_63493-9660.html

[21] M. W. E. LTD. (2019, may) MT-242021/NV/K 865 - 870 MHz, 8 dBi linear vertical polarity reader antenna. [Online]. Available: https://www.mtiwe.com/?CategoryID=255\&ArticleID=53

[22] G. R. Inc. Product overview: Solar powered UHF Gen 2 RFID tag 116421. [Online]. Available: http://www.gaorfidassettracking.com/RFID_Asset_Tracking_Products/PDF/116421.pdf

[23] C.-H. Loo, K. Elmahgoub, F. Yang, A. Z. Elsherbeni, D. Kajfez, A. A. Kishk, T. Elsherbeni, L. Ukkonen, L. Sydanheimo, M. Kivikoski *et al.*, "Chip impedance matching for UHF RFID tag antenna design," *Progress In Electromagnetics Research*, vol. 81, pp. 359–370, 2008.

[24] Impinj. (2011, may) Speedway® revolution reader application note low level user data support. [Online]. Available: http://www.buyspeedwayrevolution.com/support/Firmware/Using%20Low%20Level%20Metrics%20on%20Speedway%20Revolution.pdf

[25] R. Miesen, A. Parr, J. Schleu, and M. Vossiek, "360° carrier phase measurement for UHF RFID local positioning," in *2013 IEEE International Conference on RFID-Technologies and Applications (RFID-TA)*, 2013, pp. 1–6.